

MAGNETIC CONFINEMENT OF AN EXPANDING LASER-PRODUCED PLASMA

M. S. Tillack, S. S. Harilal, F. Najmabadi and J. O'Shay
 UC San Diego, Center for Energy Research
 9500 Gilman Drive, mail stop 0438
 La Jolla, CA 92093-0438
 mtillack@ucsd.edu

High energy ions from IFE target explosions threaten the survival and lifetime of dry chamber walls. Magnetic fields have been proposed as a possible means to divert or extract energy from the expanding plasma. We have performed experimental studies to characterize the expansion dynamics of laser ablation plumes into several magnetic field configurations, including fields aligned with or transverse to the expansion direction, and a curved field with the axis aligned with the expansion direction. Plasma was produced using pulses from a Q-switched Nd:YAG laser supplying power density in the range of 5–50 GW/cm². Significant changes were observed in the plume dynamics, including enhanced emission, confinement of the plasma, and guiding of the expansion along field lines.

I. INTRODUCTION

The idea of using magnetic fields to confine or divert high-energy ions emanating from IFE target explosions has been considered from the early days of IFE power plant research¹. It has been postulated² that a cloud of laser-produced plasma will be stopped by a magnetic field B in a distance $R \sim B^{-2/3}$. In the diamagnetic limit, applying such simple estimates indicates that a 200 MJ fusion reaction could be confined to a $\beta=1$ bubble of radius just under 5 m using a magnetic field of 1 T. In addition to confinement, the presence of a magnetic field may lead to ion acceleration, enhanced emission intensity, and various kinds of instability. Further research is needed in order to assess the feasibility of this concept and to better understand the various options and issues for magnetic confinement of IFE target emissions.

Considerable work has been performed previously on the interaction of an expanding plasma cloud with a magnetic field. Dimonte and Wiley³ investigated the expansion of plasma across a transverse magnetic field ($B=0.35$ T) and found that the plasma is contained within the magnetic cavity up to the point of peak diamagnetism. Later, the magnetic field was observed to diffuse

into the plasma anomalously fast compared to classical diffusion rates. This is believed to be caused by instability as the plasma is decelerated, and is evidenced by observations of flute structures.

Mostovych, *et. al.*⁴ investigated the expansion of laser-produced plasma in 0.5-1 T transverse magnetic fields, and reported flows that were collimated into two dimensional jets that became focused and driven unstable by the field. Even though the magnetic pressure $P_B=B^2/8\pi$ exceeded both the plasma ram pressure $P_r=nMV^2/2$ and the thermal pressure $P_t=nkT$, the jet's tip velocity was not reduced. The profile of the plasma jet in the plane normal to the magnetic field became wedge-shaped and exhibited an asymptotically narrower and denser tip.

Ripin *et. al.*^{5,6} studied sub-Alfvénic plasma expansion in the limit of large ion Larmor radius and reported that the magnetic confinement radius R_b followed the expected $B^{-2/3}$ dependency within $\pm 20\%$ error at intermediate magnetic field values. Before the plasma reached R_b , the leading edge developed distinct flute structures or spikes that projected out from the main plasma body into the magnetic field. The onset of the instability curiously occurred at about the same distance and time regardless of field strength, and the wavelengths appeared to be insensitive to the field strength as well. The experimental linear growth rate of this instability is consistent with that of the large-Larmor-radius instability theory developed by Huba *et. al.*⁷, and is nominally 6 times faster than the conventional MHD Rayleigh-Taylor growth rate.

II. EXPERIMENTAL SET-UP

Details of our experimental set-up are given in a recent publication⁸. 1.06 μ m pulses from a Q-switched Nd:YAG laser (8-ns pulse length) were used to create an aluminum plasma in a stainless steel vacuum chamber. The chamber was pumped to a base pressure $\sim 10^{-8}$ Torr. The laser beam was focused onto the target

surface at normal incidence using a plano-convex lens to achieve an average intensity of 5 GW/cm^2 over a 0.7-mm diameter spot or 50 GW/cm^2 over a 0.3-mm spot.

Plasma emission begins on the target surface soon after the laser photons reach the surface. Plume imaging was performed using an intensified CCD camera placed orthogonal to the plasma expansion direction. Visible radiation from the plasma was recorded integrally in the wavelength range 350-900 nm with 2-ns minimum gate time. A programmable timing generator was used to control the delay time between the laser pulse and the imaging system with overall temporal resolution of 1 ns. For clarity, all of the images given in the figures are normalized to the maximum intensity in that image. They are not necessarily representative of the total flux because a part of the plume is nonluminous.

An iron-core magnetic trap was fabricated to provide transverse and axial magnetic fields (see Fig. 1). NdFeB magnets ($5 \times 2.5 \times 1.5 \text{ cm}^3$) were used to generate the field in the gap. For the transverse expansion case, the separation between the magnets was kept at 1.5 cm and the target was placed 1 cm from the pole edges. In this case, the magnetic field is nearly uniform along the direction of the plume expansion with a measured maximum of 0.64 T. In the radial direction the field is less uniform.

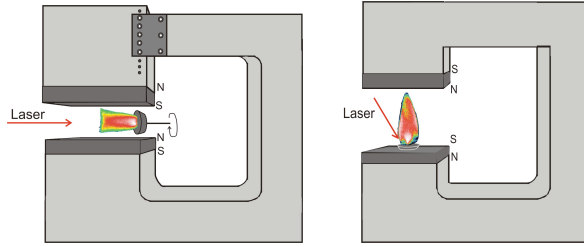


Figure 1. Schematic of the magnetic trap used for transverse and axial field experiments.

For the axial expansion case, the beam was introduced at an angle 30° with respect to the target plane. The separation between the magnets was kept at 3 cm, which provides a relatively constant 0.4 T magnetic field along the plume expansion direction.

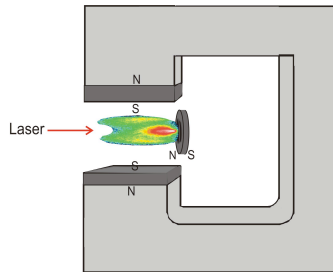


Figure 2. Schematic of the magnetic trap used for curved field experiments.

Figure 2 shows a schematic of the magnet used to study curved magnetic field configurations. We used the same neodymium magnets as above, but switched them into an opposing orientation to set up a cusp-like field. The target is mounted on a disk magnet which helps to intensify the field strength in the vicinity of the laser plasma. Plasmas were created at the center of the disk as well as 5-mm off axis.

III. PLASMA PARAMETERS

Achieving prototypical ion energies and plasma conditions which exist following an IFE target explosion requires an ignited, high-gain target facility. However, valuable information can be obtained by studying the expansion dynamics of laser ablation plumes if the parameters are similar to those of IFE expansions.

Using planar targets with beam diameter much larger than the initial plasma thickness, the expansion of a laser plasma in the absence of a magnetic field is nearly one-dimensional⁸. After termination of the pulse, adiabatic expansion is the dominant mechanism by which the plasma cools. The thermal energy is converted into directed kinetic energy of the ions, and the electron density is observed to decay exponentially. Similar behavior is seen in IFE target explosions where the initially hot (50–100 keV) dense ($10^{25}/\text{cm}^3$) plasma expands into a spectrum of high-energy ions. As the expansion proceeds, the density and temperature fall rapidly, as does the plasma beta when a magnetic field is applied. During this latter stage of the plasma expansion it is possible to simulate the expansion dynamics with laser plasma sources.

Due to the highly transient non-equilibrium nature of the plume, assignment of dimensionless parameters to describe the behavior is limited in validity. Nevertheless, we have examined several similarity parameters in order to show relevance to the IFE case. Table I summarizes parameters obtained from spectroscopic measurements at 1-mm from the target surface.

Table I. Maximum parameters achieved in an Al laser plasma formed from 8-ns, 5 GW/cm^2 pulses in a 0.64 T transverse magnetic field

Electron plasma frequency	2.4×10^{13}	Hz
Electron cyclotron frequency	1.13×10^{11}	rad/sec
Electron Larmor radius	1	μm
Debye length	20	nm
N_D	10	
Al^+ cyclotron frequency	2.3×10^6	rad/sec
Al^+ Larmor radius	1.30	cm
Alfvén velocity	4×10^5	cm/s

One of the most important parameters for expansion into a magnetic field is the plasma beta. After the initial conversion of thermal energy into directed energy, the directed β ($\beta_d = 4\pi n m V^2 / B^2$) is used. For our data in the presence of a transverse magnetic field, β_d is seen to vary by over an order of magnitude within the first 20 ns of spectral line emission (see Figure 3). Only after the plume has evolved 280 ns does β_d approach unity, indicating that the displaced magnetic field energy is approximately equal to the kinetic energy of the expanding plasma.

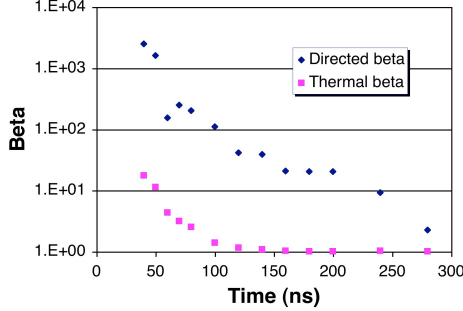


Figure 3. Time evolution of plasma beta 1 mm from the target surface

In the early phase of the plume expansion, β_d is on the order of a few thousand, which is in the regime of diamagnetic expansion.⁹ Diamagnetic currents exclude the magnetic field from the interior of the plume, and may interact with the steady state magnetic field through the $\mathbf{J} \times \mathbf{B}$ force. This dynamic will simultaneously accelerate and decelerate different regions of the plume depending on the direction of the diamagnetic currents.¹⁰

In the latter phase of the plume expansion, or non-diamagnetic limit, the plasma cools and the field is able to diffuse across the boundary relatively fast compared to the time scale of the experiment.

IV. RESULTS

IV.A. Transverse Magnetic Field

Figure 4 shows plume images at various times both with and without a transverse field applied. In the presence of magnetic field, plume propagation is considerably slowed and confined in a direction perpendicular to the target surface. The magnitude and effect of the magnetic field interaction mainly depends on the properties of the outer layer of the plume, which shields the interior of the plasma from the magnetic field¹¹. While the kinetic pressure of the plasma is greater than the magnetic pressure, the plasma penetrates through the region occupied by the magnetic field. As the plume expands, the pressure decreases and hence the resistance offered by the magnetic field increases. Plasma confine-

ment and stagnation take place when the kinetic pressure and plasma pressure balance. The confinement increases the collision frequency of the charged species both by confining them to a smaller volume and by increasing their oscillation frequency. Hence the constraint of the cross-field expansion by the magnetic field results in thermalization and a higher pressure in the confined plasma.

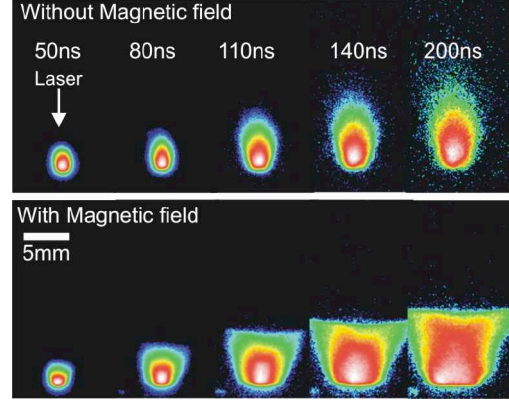


Figure 4. Plume images in the presence and absence of a transverse magnetic field.

Plume expansion in the transverse direction is significantly higher in the presence of the magnetic field, although the radial expansion velocities are much lower than the axial direction. Particles with velocity components directed only along the magnetic axis will be unaffected by the magnetic field, however we also observed transverse pressure-driven expansion across field lines. In the present studies, the lateral expansion of the plume is more pronounced at later times compared to expansion normal to the target surface.

Figure 5 shows the position-time (R - t) plot obtained from the imaging data. The symbols represent experimental data points and the curves represent the best fit. Without magnetic field the plume front expands adiabatically with a linear behavior with time (the straight-line fit in the graph corresponds to $R \propto t$).

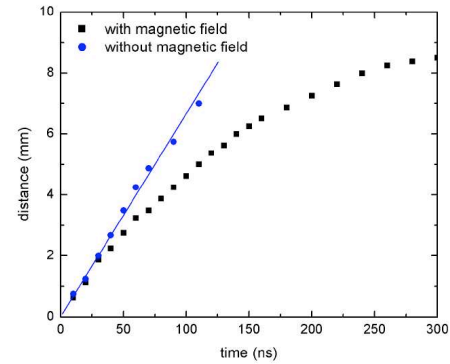


Figure 5. R - t plots obtained from plume images with and without a transverse magnetic field.

The expansion velocities of the plasmas are measured from the slopes of the displacement–time graph. The estimated expansion velocities of the plume in the field free case is 6.6×10^6 cm/s. When we introduce the magnetic trap, the plume expansion velocity dropped to 4×10^6 cm/s in the initial times and much slower at times >150 ns. The plume is never fully stopped by the magnetic field, indicating that the plume front penetrates into the magnetic field and propagates slowly.

IV.B. Axial Magnetic Field

Figure 6 shows the plume expansion in an axial magnetic field. The power density of the laser in this case was 50 GW/cm^2 . With the axial magnetic field guiding of the plasma along the field lines are observed. The images also show a collimating effect on the expanding plasma. The estimated expansion velocity of the magnetically confined plasma from the images is $\sim 4 \times 10^6$ cm/s. A secondary plasma formed on the opposing magnet also visible in the images. This may be caused by fast moving ions (velocity $\sim 10^7$ cm/s) which escaped without interacting with the magnetic field.

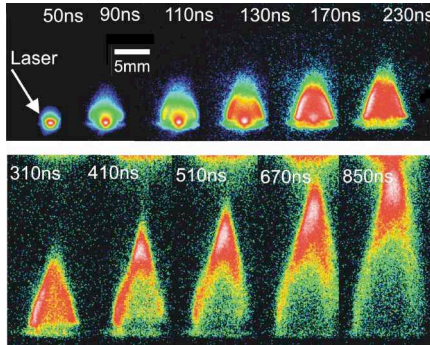


Figure 6. Plume images with an axial magnetic field.

IV.C. Curved Magnetic Field

Images of the expanding plasma with a curved magnetic field are given in Figures 7 and 8. The power density in these cases was 5 GW/cm^2 and the spot size was 0.7 mm . The images indicate that the plasma is directed along the field lines.

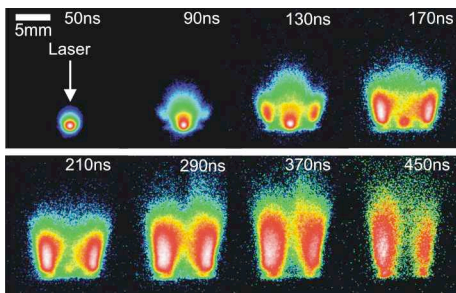


Figure 7. Images of plume expansion along the symmetry axis of a curved field.

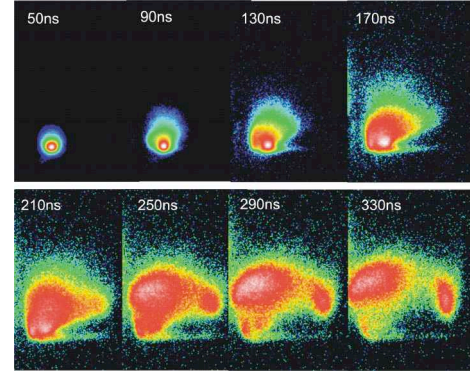


Figure 8. Images of plume expansion 5-mm off the symmetry axis of a curved field.

REFERENCES

1. L.A. BOOTH and T.G. FRANK, "Commercial Applications of Inertial Confinement Fusion," LA-6838-MS, May 1977.
2. D.K. BHADRA, "Expansion of a Resistive Plasmoid in a Magnetic Field," *Phys. Fluids* **11**, 234 (1968).
3. G. DIMONTE and L.G. WILEY, "Dynamics of Exploding Plasmas in a Magnetic Field," *Phys. Rev. Lett.* **67**, 1755-1758 (1991).
4. A.N. MOSTOVYCH, B.H. RIPIN, J.A. STAMPER, "Laser-Produced Plasma Jets: Collimation and Instability in Strong Transverse Magnetic Fields," *Phys. Rev. Lett.* **62**, 2837-2840 (1989).
5. B. H. RIPIN, E. A. MCLEAN, C. K. MANKA, C. PAWLEY, J. A. STAMPER, T. A. PEYSER, A. N. MOSTOVYCH, J. GRUN, A. B. HASSAM, and J. HUBA, "Large-Larmor-Radius Interchange Instability," *Phys. Rev. Lett.*, **59**, 2299-2302 (1987).
6. B. H. RIPIN, J. D. HUBA, E. A. MCLEAN, C. K. MANKA, T. PEYSER, H. R. BURRIS, and J. GRUN, "Sub-Alfvenic Plasma Expansion," *Phys. Fluids B*, **5**, 3491-3506, (1993).
7. J. D. HUBA, J. G. LYON, and A. B. HASSAM, "Theory and Simulation of the Rayleigh-Taylor Instability in the Limit of Large Larmor Radius," *Phys. Rev. Lett.* **59**, 2971-2974 (1987).
8. S.S. HARILAL, C.V. BINDHU, M.S. TILLACK, F. NAJMABADI, and A.C. GAERIS, "Internal Structure and Expansion Dynamics of Laser Ablation Plumes into Ambient Gases," *J. Appl. Phys.* **93**, 2380-2388 (2003).
9. T. A. PEYSER, C. K. MANKA, B. H. RIPIN, and G. GANGULI, "Electron-Ion hybrid instability in laser-produced plasma expansions across magnetic fields," *Phys. Fluids B*, **4**, 2448-2458 (1992).
10. A. NEOGI and R. K. THAREJA, "Laser-produced carbon plasma expanding in vacuum, low pressure ambient gas and nonuniform magnetic field," *Phys. Plasmas* **6**, 365-371, (1998).
11. D. W. KOOPMAN, "High-beta effects and anomalous diffusion in plasmas expanding into magnetic fields," *Phys. Fluids* **19**, 670-74 (1976).